

Figure 5.7.: a) Cross-section of the domain showing the lateral and top boundary conditions as well as the injection well and the fault zone (modified after ?).
 b) Top view on the upper aquifer showing the inner domain (30 km \times 25 km) in blue and the domain extension with an outer radius of 100 km in red. Due to the symmetry of the line connecting the injection and the fault zone only half of the domain is simulated.

5.4.1. Large-Scale Pressure Propagation During Injection

The driving force for brine migration during the injection period is the displacement of brine caused by the injected fluid. To adequately capture the far-field pressure buildup and brine leakage through the fault zone, the Zeidouni-Method is used. With this method, a reference solution is obtained for a simple test case comprising two aquifers separated by a completely impermeable layer, and connected by a vertically permeable fault zone. The model setup is illustrated in Fig. 5.7 and the relevant parameters are given in Table 5.2.

For this setting two scenarios are evaluated. The first scenario considers a closed top boundary in the upper aquifer (Neumann scenario), and the second scenario considers the upper aquifer to act as a Dirichlet boundary (Dirichlet scenario). This is achieved by increasing the permeability of the upper aquifer by several orders of magnitude, thereby increasing its diffusivity D_u ($D_u = \frac{k_u}{\mu_u \phi_u C_t}$). Here C_t is the sum of the compressibility of the porous medium and the water compressibility. The numerical model is verified against the analytical solution for different radii of the domain extension, as well as different horizontal discretization lengths. Hexahedral elements are used with a constant vertical discretization length of 50 m. The simulations are named according to their horizontal discretization length and the radius of the outer domain, for example: D300-R100 translates into a horizontal discretization length of 300 m \times 300 m and an outer radius of 100 km.

The results for the comparison of different domain lengths are shown in Fig. 5.8. Here, the leakage rates over the fault zone are plotted over time. The leakage rate is normalized by the

Table 5.2.: Input parameters for the analytical and the numerical model.
 * denotes parameters only relevant for the numerical simulation.

Parameter	Unit	Value
Injection rate	kg s^{-1}	10.87
Injection period	year	50
Injection well fault distance	m	5000
Water viscosity	Pa s	1×10^{-3}
Water compressibility	Pa^{-1}	4.5×10^{-10}
Aquifer permeabilities	m^2	1×10^{-13}
Aquifer porosities	-	0.2
Porous medium compressibility	Pa^{-1}	4.5×10^{-10}
Aquifer thicknesses	m	50
Barrier permeability*	m^2	1×10^{-25}
Barrier porosity*	-	0.001
Barrier thickness	m	50
Fault permeability	m^2	1×10^{-12}
Fault porosity*	-	0.01
Fault thickness	m	50

injection rate. The results show that for both the Neumann and Dirichlet scenario, a good

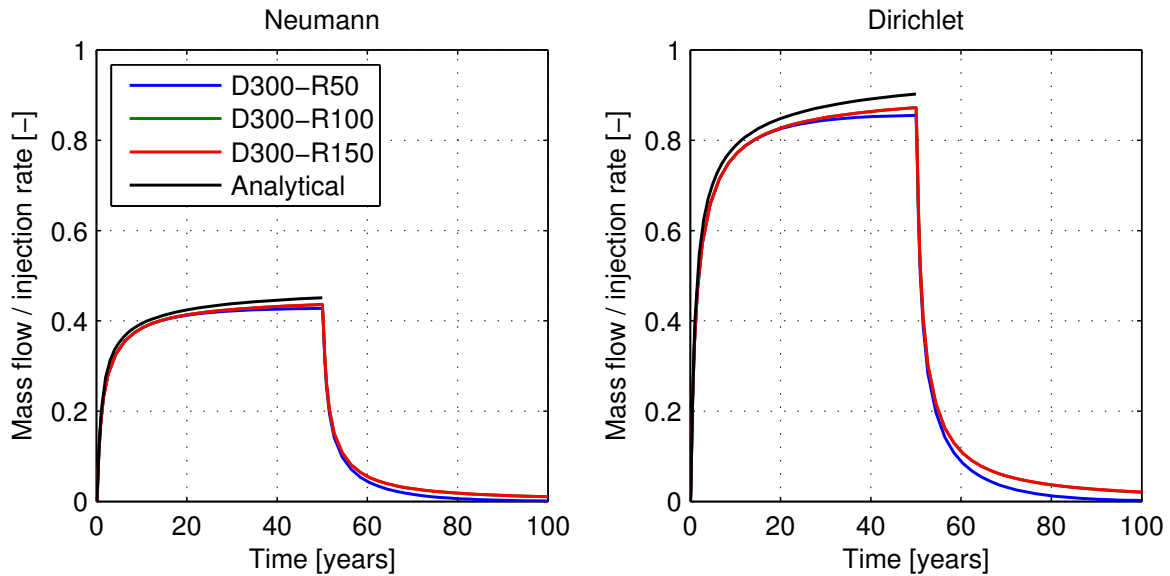


Figure 5.8.: Comparison of domain radii for 50, 100 and 150 km. **Left:** Neumann case with the upper aquifer closed on top. **Right:** Dirichlet case where the top aquifer has a constant pressure (very large diffusivity).

agreement with the analytical solution is reached for all radii. The cases for an outer radius

of 100 and 150 km are not distinguishable. The solution for the 50 km case shows a slightly smaller leakage rate. Thus, for the simulations presented below, where the complex geological model is used, an outer radius of 100 km is deemed to be sufficient.

The comparison of the different horizontal discretization lengths, for both the Neumann and the Dirichlet scenario are shown in Fig. 5.9. The results show that all three horizontal

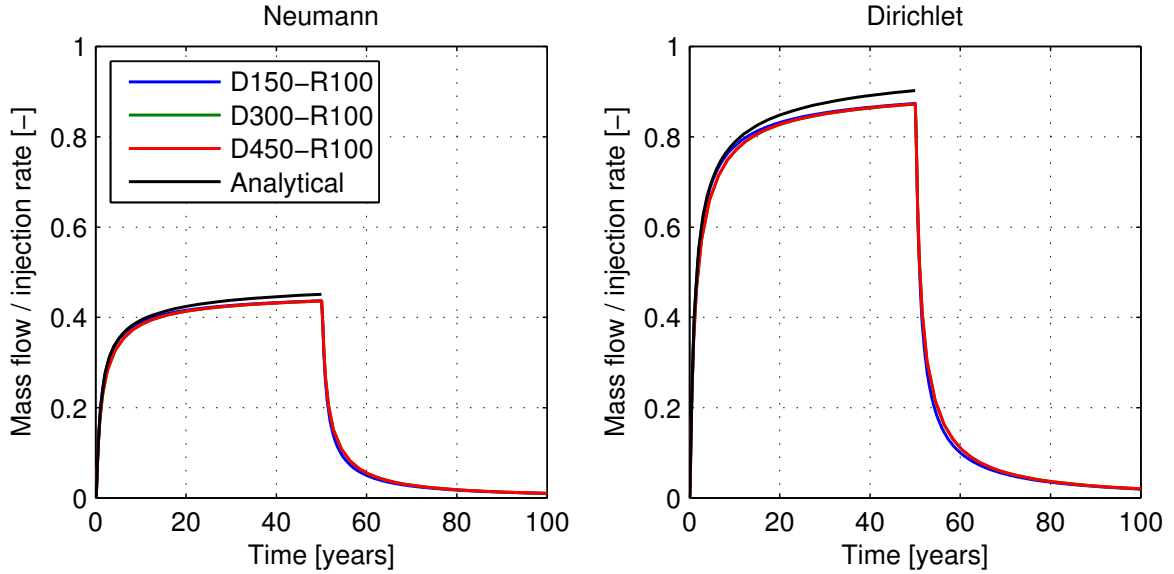


Figure 5.9.: Comparison of different horizontal discretization lengths for 150, 300 and 450 m. **Left:** Neumann case with the upper aquifer closed on top. **Right:** Dirichlet case where the top aquifer has a constant pressure (very large diffusivity).

discretization lengths sufficiently approximate the analytical solution. While the solution curves of the 300 m and 450 m discretizations are not distinguishable from each other, the solution for the 150 m case follows the analytical solution more closely. This is likely due to the strongly decreased horizontal discretization length, leading to smaller time steps, whose size is constrained by the convergence of the linear solver. A reason for the numerical simulations not exactly fitting the analytical solution may lie in the near injection region, where the relatively coarse discretization can lead to an increased numerical dispersion. However, with an outer domain radius of 100 km and a horizontal discretization length of $300\text{ m} \times 300\text{ m}$, the results are still in good agreement, with only a 3.3% deviation from the Zeidouni-Method at the end of the injection, for both the Dirichlet and the Neumann scenario. The horizontal discretization length for the complex geological model is $300\text{ m} \times 300\text{ m}$ as previously discussed in Sec. 5.2. Given the results shown here, this horizontal discretization length is a good compromise between model accuracy, the need to sufficiently resolve the geology, and the computational

feasibility.